6ICEGE 6th International Conference on Earthquake Geotechnical Engineering
1-4 November 2015
Christchurch, New Zealand

Seismic Vulnerability Assessment of RC Building Considering Soil-Structure-Interaction Effects

S.T. Karapetrou[1], S.D. Fotopoulou[2], D. Pitilakis[3]

ABSTRACT

The present study aims at the investigation of the influence of soil-structure interaction (SSI) in modifying the seismic fragility analysis of reinforced concrete (RC) structures. The consideration of SSI is achieved by applying the direct one-step coupled approach considering both linear elastic and nonlinear soil behavior. A two-step uncoupled approach is also applied to examine the relevant contribution of SSI and site effects on the structural response and fragility. A 9-story RC moment resisting frame (MRF) designed with low seismic code provisions, is adopted as a reference structure. Two-dimensional incremental dynamic analysis (IDA) is performed to assess the seismic performance of the fixed base and SSI structural systems. Fragility curves are derived as a function of outcropping peak ground acceleration (PGA) for the immediate occupancy (IO) and collapse prevention (CP) limit states.

Introduction

The assessment of seismic vulnerability of RC buildings is a prerequisite for seismic loss estimation and risk management. Currently available seismic fragility databases for RC buildings (SYNER-G Fragility Function Manager, Silva et al, 2013) are developed for fixed-based structures ignoring SSI effects. However, recent studies (Pitilakis et al., 2014) have shown that these effects might play a crucial role modifying considerably the seismic performance and fragility of RC buildings.

Although there are some studies that take into account the local site effects by providing fragility curves for buildings for different soil conditions (e.g. NIBS 2004), research on the effect of SSI to the expected structure's performance has not received much attention. This may be due to the fact that the incorporation of SSI phenomena in the analysis is generally believed to be beneficial reducing the seismic demand of linear systems. Nevertheless, it has been shown that soil deformability and SSI may modify response and fragility of non-linear structures leading to either beneficial or unfavorable effects, depending on the dynamic properties of the soil and the structure, as well as on the characteristics (frequency content, amplitude, significant duration) of the input motion (e.g. Saez et al. 2011).

Based on the above considerations, the aim of this study is to investigate further the effect of SSI on the seismic vulnerability of RC buildings. SSI is modeled by applying the direct one-step

[1]MSc, Dept. of Civil Eng., Aristotle University of Thessaloniki, Greece, gkarapet@civil.auth.gr
[2]PhD, Dept. of Civil Eng., Aristotle University of Thessaloniki, Greece, sfotopou@civil.auth.gr
[3]Assistant Professor, Dept. of Civil Eng., Aristotle University of Thessaloniki, Greece, DPitilak@civil.auth.gr

approach considering both linear elastic and nonlinear soil behavior, while site effects are inherently incorporated. To examine the relative contribution of site and SSI effects, a two-step uncoupled approach is also applied, taking into account site effects on the response of the fixed-base structure, but neglects soil-structure interaction effects. A 9-story RC MRF designed with low seismic code provisions is adopted as a reference structure. Fragility curves are derived as a function of PGA for the fixed-base (considering or not site effects) and SSI models, based on the statistical exploitation of the results of incremental dynamic analysis of the structural systems.

Selection of the prototype building model

The studied building is a nine storey – three bay RC MRF (Kappos et al. 2006) that is considered typical of high rise buildings designed according to the 1959 Greek seismic code ('Royal Decree' of 1959). In the latter regulations, the ductility and the dynamic features of the constructions are completely ignored. Table 1 presents its main characteristics, namely the total mass, the fundamental period and the strength of concrete and steel. The numerical modeling of the structure is conducted using OpenSees finite element platform (Mazzoni et al. 2009). Inelastic force-based formulations are employed for the simulation of the nonlinear beam-column frame elements. Distributed material plasticity along the element length is considered based on the fiber approach to represent the cross-sectional behavior. The modified Kent and Park model (Kent and Park 1971) is used to define the behavior of the concrete fibers, yet different material parameters are adopted for the confined (core) and the unconfined (cover) concrete. The uniaxial 'Concrete01' material is used to construct a uniaxial Kent-Scott-Park concrete material object with degraded linear unloading/reloading stiffness according to the work of Karsan-Jirsa (Karsan and Jirsa 1969) with zero tensile strength. The steel reinforcement is modeled using the uniaxial 'Steel01' material to represent a uniaxial bilinear steel material with kinematic hardening described by a nonlinear evolution equation.

Table 1. Main characteristics of the reference building

Total mass [Mg]	Initial fundamental period T [s]	fc [MPa]	fy [MPa]
334	0.89	14	400

Soil-structure-interaction modeling

The consideration of SSI is achieved by applying the direct one-step approach, which accounts simultaneously for inertial and kinematic interaction schemes. The dynamic analyses of the SSI configurations are conducted using OpenSees. The soil is modeled in two-dimensions with two degrees-of-freedom using the four-node plane strain formulation of a bilinear isoparametric quadrilateral element. To account for the finite rigidity of the underlying half-space, a Lysmer-Kuhlemeyer (Lysmer and Kuhlemeyer 1969) dashpot is incorporated at the base of the soil profile. The elastic bedrock ($V_{s,bedrock}$=900m/sec) lays at 30m beneath the ground surface. The grid adopted has a total length of 220m with a depth of 30m that includes approximately 6600 four-node quadrilateral elements. The geometry of the mesh allows an adequate number of elements to fit within the wavelength of the chosen shear wave. Considering that the maximum frequency of interest is set to 10Hz, we adopted a relatively dense discretization, with quadratic elements of 1.0m x 1.0m.

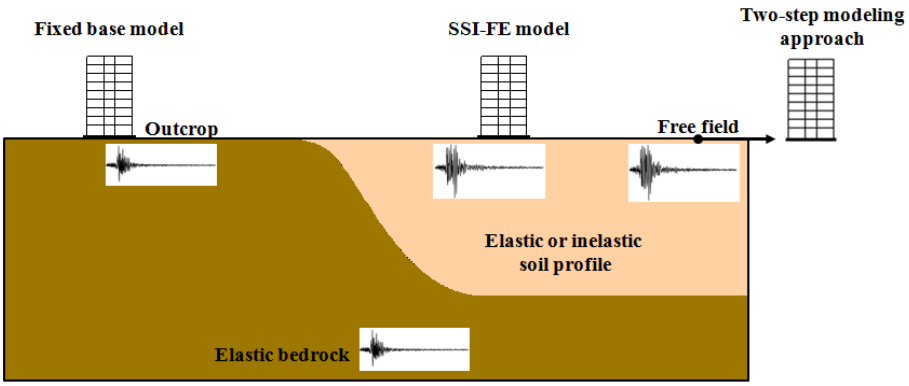

Figure 1. Schematic view of the applied modeling approaches

A first series of analyses is conducted for the fixed base structure (see Figure 1) founded on rock by imposing the outcropping bedrock input motions. To gain further insight into the influence of SSI and site effects on fragility analysis, the SSI effect considering both linear elastic and nonlinear soil behavior is investigated. For the elastic soil profile, an average shear wave velocity $V_{s,30}$ equal to 200m/s corresponding to ground type C of the Eurocode 8 soil classification system is considered. Soil nonlinearity is introduced using a pressure-independent multi yield surface incremental plasticity model with an associative flow rule with Von Mises yield surfaces (Yang et al. 2008). We consider a homogenous cohesive soil with an undrained shear strength C_u equal to 110kPa underlying the elastic half-space. In this study, a user-defined backbone curve which establishes yield surfaces and plastic shear moduli between yield surfaces is used based on the shear modulus reduction curve provided by Darendeli (2001) for clay soil with plasticity index PI=30 and atmospheric pressure p'_0 = 1atm.

Additionally, a two-step uncoupled approach is also applied in which, a 1D seismic response analysis of the given (elastic or inelastic) soil profile is first performed and then the obtained free field motion is imposed as input ground motion to the fixed base structural model. It is noted that the 1D soil profile composed of four-node quadrilateral elements using the same vertical discretization as the one used for complete 2D SSI model. This approach takes into account site effects including (or not) soil nonlinearity, but neglects SSI effects. Thus, it allows gaining further insight into the relative contribution of site and SSI effects in fragility analysis. The applied modeling approaches are presented schematically in Figure 1.

Seismic input motion

The selected scenario earthquake consists of a set of 15 real ground motion records obtained from the European Strong-Motion Database (http://www.isesd.hi.is) (Pitilakis et al. 2014). They are all referring to outcrop conditions recorded at sites classified as rock according to EC8 (soil type A) with moment magnitude (M_w) and epicentral distance (R) that range between $5.8<M_w<7.2$ and $0<R<45$km respectively. Outcropping records are selected to avoid uncertainties related to soil effects. Additionally in order to eliminate potential source of bias in structural response, the selection of pulse-like records has been avoided. The primary selection criterion is the average acceleration spectra of the set to be of minimal “epsilon” (Baker and Cornell 2005) at the period range of $0.00<T<2.00$sec with respect to a reference spectra defined

based on the ground motion prediction equation (GMPE) proposed by Ambraseys et al. (1996) corresponding to the median of the M_w and R selection bin. The optimization procedure is performed by making use of the REXEL software (Iervolino et al. 2010). Figure 2 depicts the mean normalized elastic response spectrum of the records in comparison with the corresponding median predicted spectrum of Ambraseys et al. (1996). As shown in the figure, a good match between the two spectra is achieved.

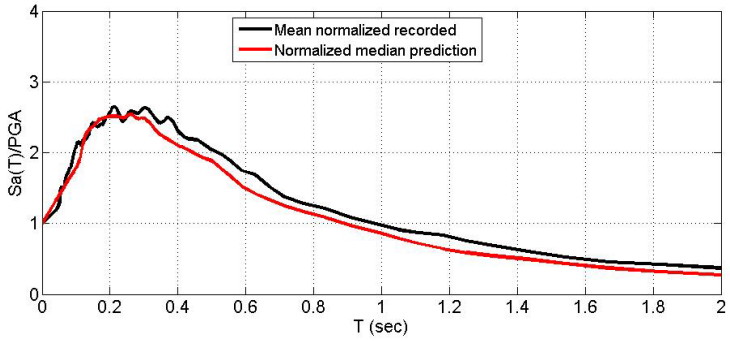

Figure 2. Normalized average elastic response spectrum of the input motions in comparison with the corresponding reference spectrum proposed by Ambraseys et al. (1996)

Incremental dynamic analysis

Incremental dynamic analysis (Vamvatsikos and Cornell 2002) is performed to assess the seismic vulnerability of the given structure under the influence of SSI and site effects. The damage measure is expressed in terms of maximum interstory drift ratio (maxISD) while the seismic intensity is described using peak ground acceleration (PGA) recorded on rock outcropping or soil type A according to EC8. IDA for the fixed base and soil-structure models is conducted by applying the 15 progressively scaled records. A PGA-stepping algorithm is used to perform the IDA comprising a first elastic run at 0.005g and an initial step of 0.1. The minimum number of converging runs is allowed to vary from 8 to 12 per record depending on the characteristics of the structure and the record itself. By interpolating the derived pairs of PGA and maxISD for each individual record we get 15 continuous IDA curves for each structural model. Figure 3 presents the graphs of the derived IDA curves for each record in terms of PGA and the corresponding summarized across all records IDA curves at 16%, 50% and 84% fractiles for the fixed base structure.

Next step is the definition of the limit values of the damage states for the derivation of seismic fragility curves. Two limit states are selected in terms of maximum interstory drift ratio, maxISD, representing the immediate occupancy (IO) and collapse, or near collapse prevention (CP) performance levels. The first limit state is defined at 0.5% according to HAZUS prescriptions (NIBS 2004) for RC MRF structures designed with low code seismic provisions, whereas the second is assigned on the median (50%-fractile) IDA curve derived in terms of PGA (see Figure 3). The main idea is to place the CP limit state at a point where the IDA curve is softening towards the flat line but at low enough values of maxISD so that we still trust the structural model (Vamvatsitkos and Cornell 2004). The CP limit is selected equal to 0.0225.

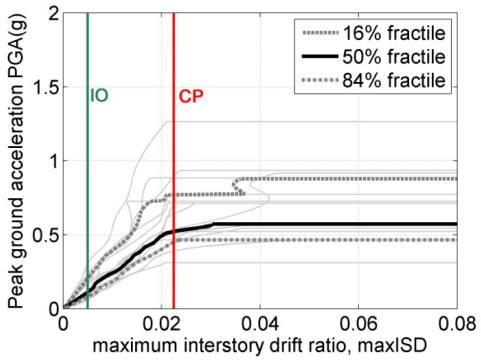

Figure 3. IDA curves for the fixed base building model

Fragility curves

A fragility curve represents a graphical relationship of the probability of exceeding a predefined level of damage (e.g. IO, CP) under a seismic excitation of a given intensity. Equation 1 gives the cumulative probability of exceeding a *DS* conditioned on a measure of the seismic intensity *IM*.

$$P\left[DS / IM\right] = \Phi\left(\frac{In\left(IM\right) - In\left(\overline{IM}\right)}{\beta}\right) \tag{1}$$

where Φ is the standard normal cumulative distribution function, *IM* is the intensity measure of the earthquake expressed in terms of PGA (in units of *g)*, $\overline{IM}$ and β are the median values (in units of *g)* and log-standard deviations respectively and *DS* is the damage state. The median PGA values corresponding to the prescribed performance levels are determined based on a regression analysis of the nonlinear IDA results (PGA- maxISD pairs) for each structural model. Figure 4 presents comparative PGA - maxISD diagrams of the structure considering SSI and fixed base models under linear and nonlinear soil conditions respectively. It is worth noting that while for the linear elastic soil behavior the fixed base model tends to yield higher interstory drift ratios compared to the SSI model for PGA level lower than approximately 0.5g, when soil nonlinearity is considered these results are reversed with the nonlinear SSI model presenting higher drift values for the entire PGA level range.

The various uncertainties are taken into account through the log-standard deviation parameter β, which describes the total dispersion related to each fragility curve. Three primary sources of uncertainty contribute to the total variability for any given damage state (NIBS 2004), namely the variability associated with the definition of the limit state value, the capacity of each structural type and the seismic demand. The log-standard deviation value in the definition of limit states is assumed to be equal to 0.4 while the corresponding value in the capacity is assumed to be 0.3 for low code structures (NIBS 2004). The third source of uncertainty associated with the demand, is taken into consideration by calculating the dispersion of the logarithms of PGA - maxISD simulated data with respect to the regression fit. Under the assumption that these three log-standard deviation components are statistically independent, the

total log-standard deviation is estimated as the root of the sum of the squares of the component dispersions. The herein computed log-standard deviation β values of the curves vary from 0.62 to 0.75 for all structural models.

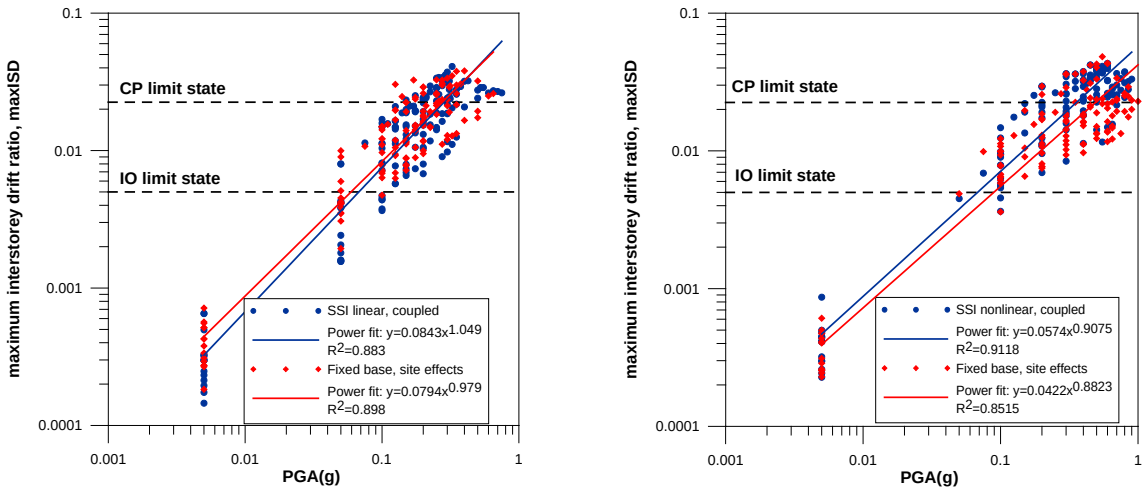

Figure 4. Comparative PGA - maxISD relationships for the SSI and fixed base models under linear (left) and nonlinear (right) soil behaviour

Table 2. Parameters of the fragility functions in terms of PGA for the considered structural configurations

RC building	**Median PGA (g)**		**Dispersion β**
	IO	**CP**	
Fixed base, rock	0.14	0.68	0.65
SSI linear, coupled	0.07	0.28	0.68
Fixed base, linear site effects	0.06	0.28	0.65
SSI nonlinear, coupled	0.07	0.36	0.64
Fixed base, nonlinear, site effects	0.089	0.50	0.75

The derived fragility for the fixed base, structure have been compared with the literature and have been found to be in good agreement verifying the reliability of the proposed fragility functions for the initial as built state. More details regarding the validation results can be found in Pitilakis et al. (2014).

Table 2 presents the lognormal distributed fragility parameters (median and log-standard deviation) in terms of PGA for the buildings considering fixed base conditions and SSI configurations. Figure 5 depicts the comparative plots of fragility curves for the different SSI configurations compared to the reference fixed base model without modifying the ground motion due to site effects. It is shown that the SSI model, which considers soil nonlinearity is less vulnerable compared to the SSI system where linear elastic soil behaviour is taken into account. This observation is more noticeable for the CP damage limit state. Nevertheless, a significant overall increase of the building's fragility with respect to the fixed base model founded on rock is still shown. In Figure 6 we compare the fragility curves for the different coupled SSI cases and fixed base models considering linear elastic and inelastic soil behavior. We observe an important

difference between the linear elastic and non-linear case. When soil behavior is assumed linear elastic the coupled approach, where SSI and site effects are considered inherentley, has practically no difference with the uncoupled fixed base model where site effects are taken into account. On the other hand, when soil non-linearity is taken into consideration then the coupled case of SSI and site effects leads to a significant increase of the vulnerability compared to the fixed base case where site effects are taken into account through the 1D analysis. A possible explanation is that nonlinear soil behavior introduces additional translation and rotation effects and thus increased displacement demands to the structure.

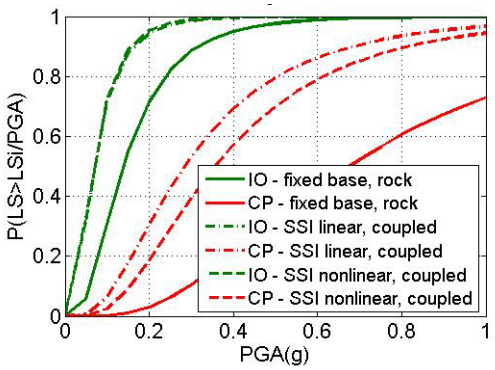

Figure 5.Fragility curves for the fixed base structure founded on rock and the SSI structural configurations under linear and nonlinear soil behavior

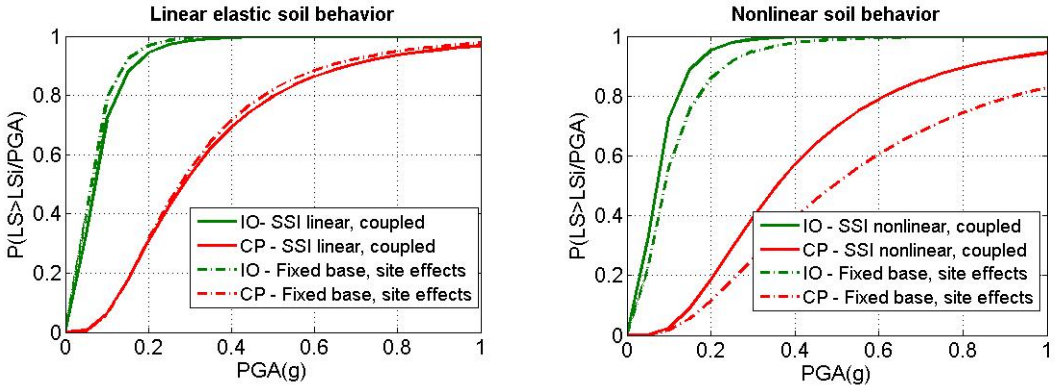

Figure 6. Fragility curves for the fixed base structure considering site effects and the SSI structural configurations under linear (left) and nonlinear (right) soil behavior

Conclusions

The seismic vulnerability of a high rise RC frame building designed with low seismic code provisions has been assessed taking into account soil-structure interaction. The consideration of site and SSI effects may significantly affect the performance of a RC structure founded on rather soft soil conditions, increasing considerably the vulnerability of the structure compared to the reference case where the structure is supposed as fixed base and no SSI or site effects are taken into account. When soil nonlinearity is introduced these effects are generally expected to be

lower for higher levels of seismic loading.When soil behavior is assumed linear elastic the coupled SSI approach has practically no difference with the uncoupled fixed base model where site effects are taken into account. On the other hand, nonlinear SSI leads in an increase of the structure's vulnerability in comparison to the corresponding fixed base model which may be attributed to the complex nonlinear behavior of the underlying soil that may introduce additional translation and rotation effects to the structure yielding to higher displacement demands. Both modeling approaches, however, produce higher vulnerability values compared to the reference fixed base structure founded on rock. Overall, the present study provides a further insight on the seismic vulnerability of typical RC frame buildings by proposing fragility functions applicable to a variety of RC typologies exposed to SSI effects. It is seen that the soil properties and SSI effects may play a crucial role in the expected structural damage and therefore they should not be neglected for assessment purposes. Given the significance of the SSI and site effects in the structure's vulnerability, future work should also address the investigation of SSI in relation to soil and foundation compliance with different soil conditions.

Acknowledgements

We would like to thank the support provided by the General Secretariat for Research and Technology, Greece (Grant No: 11ΣΥΝ_8_1577, ESPA 2007-2013).

References

Ambraseys NN, Simpson KA, Bommer JJ (1996) Prediction of horizontal response spectra in Europe, *Earthquake Engineering and Structural Dynamics*; **25**: 371-400

Baker JW, Cornell CA. A vector valued ground motion intensity measure consisting of spectral acceleration and epsilon. *Earthquake Engineering and Structural Dynamics* 2005; **34**:1193-1217.

Darendeli M. *Development of a new family of normalized modulus reduction and material damping curves*. Ph.D. Dissertation, Univ. of Texas, 2001.

Iervolino I, Galasso C, Cosenza E. REXEL: Computer aided record selection for code-based seismic structural analysis. *Bulletin of Earthquake Engineering* 2010; **8**:339-362

Kappos AJ, Panagopoulos G, Panagiotopoulos C, Penelis G. A hybrid method for the vulnerability assessment of R/C and URM buildings. *Bulletin of Earthquake Engineering* 2006; **4**:391-419

Karsan I, Jirsa J. Behavior of concrete under compressive loadings. ASCE *J. of the Structural Division* 1969; **95**: 2543-2563

Kent DC, Park R. Flexural members with confined concrete. *Journal of the Structural Division*. Proc. Of the American Society of Civil Engineers 1971; **97** (ST7): 1969-1990.

Lysmer J, Kuhlemeyer RL. Finite dynamic model for infinite media. *Engineering Mechanics* 1969; **95**: 859-877.

Mazzoni S, McKenna F, Scott, MH, Fenves GL. *Open System for Earthquake Engineering Simulation User Command-Language Manual*. Pacific Earthquake Engineering Research Center, Berkeley, California, 2009.

National Institute of Building Sciences. *Direct physical damage – General building stock. HAZUS-MH Technical manual*, Chapter 5. Federal Emergency Management Agency, Washington, D.C., 2004.

Pitilakis K, Karapetrou ST, Fotopoulou SD. Consideration of aging and SSI effects on seismic vulnerability assessment of RC buildings. *Bulletin of Earthquake engineering* 2014; **12** (4): 1755-1776.

Saez E, Lopez-Caballero F, Modaressi-Farahmand-Razavi A. Effect of the inelastic dynamic soil-structure interaction on the seismic vulnerability assessment. *Structural Safety* 2011; **33**: 51-63

Silva V, Crowley H, Colombi M. *Fragility Function Manager, version 2.0*, Seventh Framework Program (FP7): SYNER-G: Systemic Seismic Vulnerability and Risk Analysis for Buildings. Lifeline Networks and Infrastructures Safety Gain, 2011.

Vamvatsikos D, Cornell CA. Incremental dynamic analysis. *Earthquake Engineering and Structural Dynamics* 2002; **31**:491-514.

Vamvatsikos D, Cornell CA. Applied incremental dynamic analysis. *Earthquake Spectra* 2004; **20** (2): 523-553.

Yang Z, Lu J, Elgamal A. *OpenSees Soil Models and Solid- Fluid Fully Coupled Elements*, User's Manual, 2008 ver 1.0. University of California, San Diego, 2008.